Technology Section

Pak. j. sci. ind. res., vol. 38, no. 3-4, March-April 1995

A NUMERICAL MODEL FOR THE TIDES OF THE PAKISTANI COASTAL WATERS

KHAWAJA ZAFAR ELAHI

Mathematics Department, College of Science, King Saud University, P.O.Box 2455, Riyadh 11451, Saudi Arabia

(Received July 4, 1993 ; revised October 2, 1994)

Tidal processes in the Pakistani coastal area are studied by using the mathematical tools. A two-dimensional explicit finite difference hydrodynamical numerical technique is used for reproduction of harmonic constants of the tidal constituents M_2, S_2, K_1 and O_1 -Tide, in the area. A variable finite difference method is discussed. The area of interest is being convered with a finer grid, whereas a coarser grid is taken in the rest of the model. The results are presented in the form of co-range and co-tidal charts. Values of amplitudes and phases at important coastal points are given in form of a table.

Key words: Numerical model, Tidal dynamics, Pakistani coastal.

Introduction

Hydrodynamical numerical model capable of simulating tidal dynamics has been applied to near shore coastal areas. The knowledge of the tidal dynamics, tidal currents, and tidal elevation constitute a major part of the information required for the development of the coastal structures and navigation. The model developed can be used to study the flow dynamics with exceptional and rare events and to investigate with higher accuracy the influence of the constructional alternatives on the tidal dynamics. Such information, is however, used as the criteria for design in coastal engineering problems. The data on currents can be used for computing stresses on constructions, erosion and deposition of sediments and for evaluation of the transport and distributions of substances such as pollution.

Tidal dynamics of the Indus delta (Fig. 1), situated at the north of the Arabain Sea, is being studied. The water movement in the sea is dominated by the tides. These are of mixed type with a dominating semi-diurnal components. Principal partial tide M_2, S_2, K_1, and O_1 will be studied. No observational data is available in the open sea area under study, hence generation of the tide on the open boundaries depend only on results of the nested model for the tides of the northern Arabian Sea (Fig.1).

The bathmetry of the Pakistani coastal area (Fig.2) is based on Chart No.746 of the German Hydrogarphic Institute, Hamburg. The area includes one of the world oldest port Karachi and Indus delta. Indus delta is the area for possible extension of the navigational activities. A newly built Pakistani second major port, Qasim Port, is situated in Kadiro Creek of the Indus delta. The model area is very shallow with average water depth of 40 meters. Depth varies from 3 metes in the Indus delta to 66 meters in the open sea area.

Variable finite difference scheme. A square grid is used for the computation by finite difference method. The time interval is restricted by the Courant Friedriches-Lewy

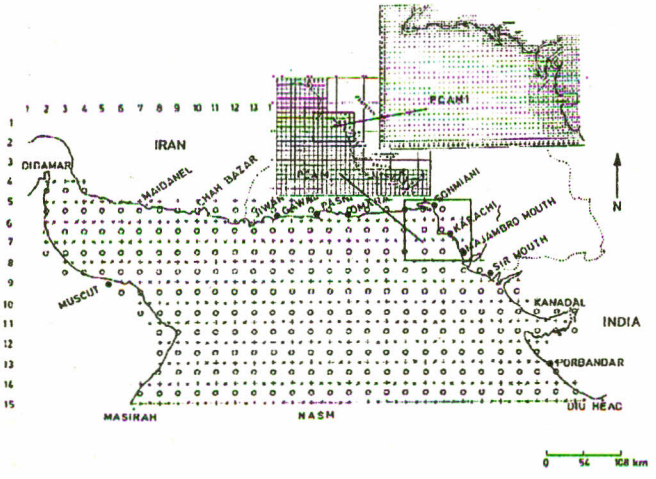

Fig. 1. Hiderarchy of nested models from the northern Arabian Sea to the Pakistani Coastal Area.

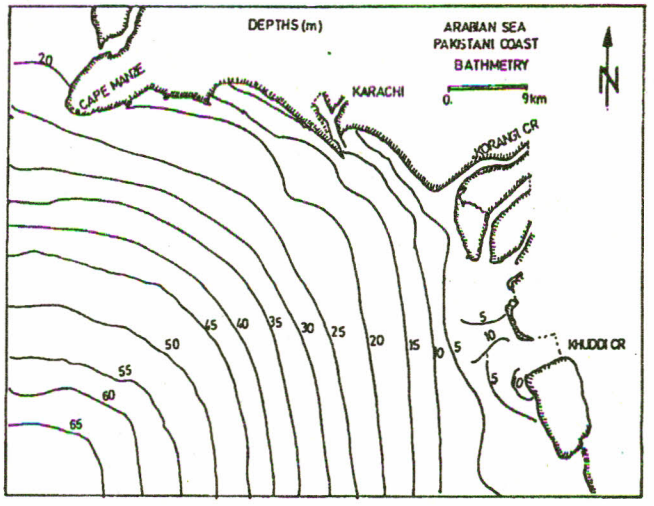

Fig. 2. Bathmetry of the Pakistani Coastal Area.

(CFL-) stability criterion. A small finite mesh size required small time interval and many computational points. This short coming is overcome by considering a finer mesh size in the region of interest and a coarser mesh size in rest of the region. Numerical experiments were performed to reproduce the tidal dynamics by taking each portion separately and a single model with meshes of different sizes [1]. It was found that one can save computation time effort by computing each finer model separately without loss of accuracy. In this scheme, the results of previously computed model were taken as the boundary values for the finer model. These models (Table 3) produced data for generation of tide and to check the reproduction ability of the numerical model with completion of the present study, a set of models of the area with the mesh size reducing for 54 km to 1.8 km is achieved. The results of the northern Arabian Sea Model (NASM) with mesh size 54 km are discussed by Elahi and Shaifque [2]. NASM 1 is model with mesh size 18 km, which is one third of previous model. Principal partial tides and their combined effect are studied through a model of Pakistani coastal area [PCAM] with mesh size of 9 km [3]. In the present study [PCAM1], the mesh size is further reduced to 1.8 km that is one fifth of the previous model [Fig.1].

Mathematical model of the Pakistani coastal area. The system of equations which describes the tidal dynamics of large fluid masses is derived from the Navier-Stokes equation of motion and equation of continuity. Since water movements are mainly horizontal and horizontal dimensions are much greater than the depth, thus the systme is vertically integrated over depth and has been simplified to a two-dimensional system. The system includes effects of the bottom friction, rotation of the earth and the atmospheric pressure gradient. The tide in the model is generated by prescribing the water-level variation as a function of time of the open boundaries.

$$\frac{\partial \zeta}{\partial t} + \frac{1}{R \cos \phi}\left[\frac{\partial}{\partial \lambda}(h+\zeta)u + \frac{\partial}{\partial \phi}(h+\zeta)v \cos \phi\right] = 0 \quad \ldots (1)$$

$$\frac{\partial u}{\partial t} - \Omega v + \frac{\tau_b^{\lambda}}{h+\zeta} - A_h \nabla^2 u + \frac{g}{R \cos \phi}\frac{\partial \zeta}{\partial \lambda} = 0 \quad \ldots (2)$$

$$\frac{\partial u}{\partial t} - \Omega v + \frac{\tau_b^{\phi}}{h+\zeta} - A_h \nabla^2 v + \frac{1}{R}\frac{\partial \zeta}{\partial \lambda} = 0 \quad \ldots (3)$$

If u(z) and v(z) denote the horizontal velocity components at depth z below the undisturbed sea level, the:

$$u = \frac{1}{h+\zeta}\int_{-h}^{\zeta} u(z)\, dz \quad \ldots (4)$$

$$v = \frac{1}{h+\zeta}\int_{-h}^{\zeta} v(z)\, dz \quad \ldots (5)$$

The system includes the Corilols force Ω, which results from the fact that our reference system is fixed to the earth, but the earth itself is moving through the space. The effects in horizontal plane are consiered only:

$$\Omega = 2\,\omega \sin \phi \quad \ldots (6)$$

It acts as an external force much in the manner of the gravitational fore.

In shallow water, at the bottom a 'no-slip' boundary condition does not specify the bottom stress. An alternative form of bottom boundary condition is to specify the bottom stresses in terms of the flow field. It is parametrized empirically by using the Newton - Taylor formulation:

$$\tau_b^{\lambda} = r u (v^2 + v^2)^{1/2} \quad \ldots (7)$$

$$\tau_b^{\phi} = r v (u^2 + v^2)^{1/2} \quad \ldots (8)$$

where r = .003 is the bottom friction coefficient.

Shear stresses arises from turbulent stresses, which are caused by "chunks" of fluid moving back and forth and exchanging momentum with surrounding fluid. The effect of viscous friction is included through terms with the coefficient of horizontal eddy viscosity A_h:

$$A_h = \frac{1 - \alpha (\Delta l)^2}{4\ \Delta t} \quad \ldots (9)$$

α takes value between 0.9 and 0.99, depending upon then inner viscosity of the fluid [4]. Through numerical experimental, its numerical value is estimated 0.99 in the shallow water and 0.90 in the deep water areas.

The following notations have been used

U,V = Compnents of vertically averaged velocity in the λ and ϕ directions, resp. [ms^{-1}].
ζ = Water elevation [m]
A_h = Coefficient of horizontal eddy viscosity [$m^2\ s^{-1}$]
g = Acceleration due to gravity [ms^{-2}]
h = Mean water depth [m]
r = Bottom friction coefficient
R = Radius of the Earth [m]
t = Time [s]
λ,ϕ = Geographical longitude and latitude
Ω = Angular velocity of the Earth's rotation [s^{-1}]

∇^2 = Horizontal Laplacian operator [$1/m^{-2}$]

Initial and boundary conditions. The solution of the above equations require the knowledge of initial and boundary conditions. Because of the frictional dissipation, the damping rate of any disturbance is particularly high, so after two or three tidal periods the influence of initial conditions becomes negligible in comparison with effects produced by the generating forces. So the tides are generated from initial state of rest.

$$\zeta = U = V = 0 \text{ at } t = 0 \quad \ldots\ldots (10)$$

There are two types of boundaries in the model, coastal line is treated as solid boundary and supposed joining line of the modelled area with the main sea is treated as open sea boundary.

On the solid boundary no-slip condition is true.

$$u = v = 0 \quad \ldots\ldots (11)$$

On the open sea boundaries water elevations are prescribed at every time step by using

$$\zeta(t) = A\cos(\sigma t - k) \quad \ldots\ldots (12)$$

where A is amplitude, k is the phase of incoming tide and σ is the frequency of the partial tide on boundary. The necessary velocity values are approximated on assumption of quasi-uniformity of the velocity across the boundary i.e.,

$$\frac{\partial V}{\partial n} = 0 \quad \ldots\ldots (13)$$

On the open boundaries, where the data is not available to prescribed water elevation by using Eq (12), the water elevations are approximated on assumption of quasi-uniformity of the water elevations across the boundary i.e.

$$\frac{\partial \zeta}{\partial n} = 0 \quad \ldots\ldots (14)$$

Explicit finite difference method. The system of partial differential equations (Eq. 1-3) with the initial and bounary conditions (Eq. 10, 13) is transformed into a set of algebraic equations by using forward difference for time derivatives and centered difference for space derivative. The computation of ζ value at , $t + \delta t/2$; time level involve known values of U and V at 't' time level and value at $t-\Delta t/2$ time level. The computation of U and V values at '$t + \Delta t$' time level involves known values of U and V at 't' time level and newly computed value at ' $t + \Delta t/2$' time level.

The functional form of the algorithm is :

$$\zeta^{t+\Delta t}(N, M) = f_1(\zeta^{t-\Delta t/2}, U^t, V^t) \quad \ldots\ldots (15)$$

$$U^{t+\Delta t}(N, M) = f_2(\zeta^{t+\Delta t/2}, U^t, V^t) \quad \ldots\ldots (16)$$

$$V^{t+\Delta t}(N, M) = f_3(\zeta^{t+\Delta t/2}, U^t, V^t) \quad \ldots\ldots (17)$$

Transformed set of algebraic equations under the explicit

$$U^{(t+\Delta t)}(N, M) = \left(1 - r\Delta t \frac{U^{(t)}(N, M)^2 + V_u^{(t)}(N, M)^2}{HU^{(t)}(N, M)}\right) U(N, M) + 2\omega\Delta t \sin(\phi(N) V_u^{(t)}(N, M) + A_h \Delta t \nabla^2 U^{(t)}(N, M) + g\Delta t \frac{\zeta^{(t+\Delta t/2)}(N, M) - \zeta^{(t+\Delta t/2)}(N, M+1)}{R\cos(\phi(N))} \quad \ldots\ldots (18)$$

$$U^{(t+\Delta t)}(N, M) = \left(1 - r\Delta t \frac{V^{(t)}(N, M)^2 + U_u^{(t)}(N, M)^2}{HV^{(t)}(N, M)}\right) V(N, M) - 2\omega\Delta t \sin(\phi(N) U_u^{(t)}(N, M) + A_h \Delta t \nabla^2 V^{(t)}(N, M) - g\Delta t \frac{\zeta^{(t+\Delta t/2)}(N, M) - \zeta^{(t+\Delta t/2)}(N+1, M)}{R\Delta\phi} \quad \ldots\ldots (19)$$

$$\zeta^{(t+\Delta t/2)}(N, M) = \zeta^{(t-\Delta t/2)} + \frac{\Delta t}{R\cos(\phi(N))} \times \frac{HU(N^t, M)^{(t)}(N, M) - HU^{(t)}(N, M-1)U^{(t)}(N, M-1)}{\Delta\lambda} - \frac{HV(N^t, M) V^{(t)}(N, M)\cos(\phi(N) - \frac{\Delta\phi}{2}) HV(N^{(t)} - 1, M) V^{(t)}(N-1, M)\cos(\phi(N-1)}{\Delta\phi} \quad \ldots\ldots (20)$$

where

$$HU^{(t)}(N,M) = hU(N,M) + \tfrac{1}{2}(\zeta^{(t-\Delta t/2)}(N, M) + \zeta^{(t-\Delta t/2)}(N, M+1)) \quad \ldots\ldots (21)$$

$$HV^{(t)}(N, M) = hv(N,M) + \tfrac{1}{2}(\zeta^{(t-\Delta t/2)}(N, M) + \zeta^{(t-\Delta t/2)}(N, M+1)) \quad \ldots\ldots (22)$$

$$H_v^{(t)}(N, M) = \tfrac{1}{4}(U(N^{(t)}, M-1) + U(N^{(t)}, M-1) + U(N^{(t)}, M) + (U+1, M-1) + U^{(t)}(N+1, M)) \quad \ldots\ldots (23)$$

$$H_u^{(t)}(N, M) = \tfrac{1}{4}(V(N^{(t)}, M-1) + V(N^{(t)}, M) + V(N-1, M+1) + V^{(t)}(N-1, M)) \quad \ldots\ldots (24)$$

$$\nabla^2 U \approx \frac{1}{\Delta l^2}(U^{(t)}, (N-1, M) + U^{(t)}(N+1, M) + U^{(t)}(N, M+1) + U^{(t)}(N, M-1) - 4^{(t)} U(N, M) \quad \ldots\ldots (25)$$

$$\nabla^2 V \approx \frac{1}{\Delta l^2}(VN^{(t)} - 1, M) + V^{(t)}(N+1, M) + V^{(t)}(N, M+1) + V^{(t)}(N, M-1) - 4^{(t)} V(N, M) \quad \ldots\ldots (26)$$

where

$$\Delta l = R\Delta\phi$$

Solutions are found on a staggered grid, with variables defined in rectrangular grid boxes of dimensions $\Delta\phi$ and $\Delta\lambda$ (Fig. 3). The water level points ζ are located at the middle of a box and velocity components U and V are located on meridional and zonal edges of the boxes respectively.

For this method an efficient time step is required for numerical stability and is simply the time required for a point in the fluid to move over a specific distance $\Delta 1$. It is obtained by using the Corant-Friedriches-Lewy stability condition [5], which ensure that the physical velocity is less than its mesh speed

$$\Delta t \leq \frac{\Delta l}{\sqrt{2gh_{max}}} \quad \text{.....(27)}$$

where Δl is the mesh size and h_{max} is the maximum water depth in the area.

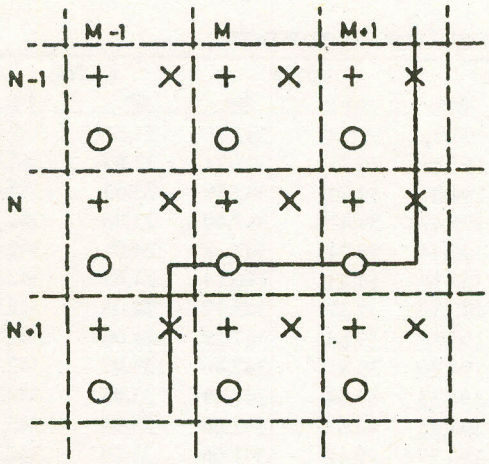

Fig. 3. Hydrodynamical-Numerical Grid.

Results and Discussion

The set of explicit finite difference equations (Eq. 17-27) have been evaluated numerically by using the hydrodynamical-numerical method [6]. Program was written in FORTRAN IV. Computations were done on personal computer 386-DX 33 with RM/FORTRAN compiler. The PC includes the Math coprocessor 80387 and a Harddisk of 40 MB. Graphic work was one by using Geograf Fortran Ver 4.0.

The following output has been obtained.

(a) Maximum value of the difference between the tidal elevation in consecutive tidal cycles were printed to check the convergence of the technique.

(b) The values of tidal elevation and velocity components for the whole region were printed at an interval of quarter of the period of the partial tide for the last tidal period of computation.

(c) Magnitude and direction of the velocity field were computed, printed and plotted by using the velocity components.

$$|V| = \sqrt{u^2 + v^2} \quad \text{.....(28)}$$

$$\psi = \arctan \frac{v}{u} \quad \text{.....(29)}$$

(d) The local tidal amplitude is defined as half the "tidal range' which measures the tidal variation of the waterlevel from high to low. The local phase specifies the tidal cresting time (in degree) after the Sun's passage over the greenwich meridian. Amplitude and phases for the whole region were computed, printed and plotted by using quarterly computed waterlevels.

$$\zeta(t) = A\cos(\sigma t + \kappa)$$
$$= \zeta_1 \text{ Cost} + \zeta_2 \sin t \quad \text{.....(30)}$$

$\zeta_1 = A \cos \sigma t$ is a waterlevel at the beginning of the first quarter of tidal period (T).

$\zeta_2 = A \sin \sigma t$ is a waterlevel at the beginning of second quarter of the tidal period (T + T/4). Thus, amplitude

$$A = \sqrt{\zeta^2_1 + \zeta^2_2} \quad \text{and phase.....(31)}$$

$$\kappa = \arctan \frac{\zeta_2}{\zeta_1} \quad \text{.....(32)}$$

Amplitude and phases. Charts have been constructed for each partial tide (Table 4) containing lines of equal amplitudes 'Co-range line' (in cm) and of euqal phases 'Co-tidal line' (in degree). Tidal charts for the four major partial tides M_2, S_2, K_1

TABLE 1. MAXIMUM DIFFERENCES AT FOUR COASTAL POINTS (TABLE 6).

Tide	Amplitude (cm)	Phase (deg)
M_2	2.45	1.34
S_2	0.91	4.01
O_1	0.42	1.86
K_1	0.12	0.80

TABLE 2. COMPARISON OF OBSERVED AND COMPUTED VALUES AT KARACHI.

Tide		Observed	Computed	Difference
M_2	a	79.8	81.22	1.42
	k	163.7	167.33	3.63
S_2	a	29.6	33.36	3.76
	k	193.9	194.86	0.96
K_1	a	40.0	39.84	0.16
	k	341.0	347.49	6.49
O_1	a	24.0	23.97	0.03
	k	342.0	342.75	0.75

TABLE: 3. MODELS PARAMETERS.

Model	Starting Position N	E	Model Size	Grid Size ΔX [km]	Time interval Δt [sec]	Max Water Depth [M]	Horizontal Eddy Viscosity[Cm²/Sec]
NASM	56°.00'	27°.40'	15 x 30	54	150	3550	.1 x 10^{10}
NASM1	62.50	25.50	10 x 27	18	60	3000	.1 x 10^{9}
PCAM	66.00	25.47	26 x 30	9	90	500	.135 x 10^{9}
PCAM	66.32	24.50	27 x 41	1.8	45	70	.165 x 10^{9}

NASM - Northern Arabian Sea Model, PCAM - Pakistani Coastal Area Model.

TABLE: 4. CHARACTERISTICS OF MAJOR TIDE - PRODUCING FORCES CONSTITUENTS.

Specics and Name	Symbol	Period solar hours	τ (o/h) hour angles	Frequency σ 10^{-4}/S	Relative Size
Semi - diurnal tide					
Principal lunar	M_2	28.98410	12.42	1.40519	100
Principal solar	S_2	30.00000	12.00	1.45444	47
Diurnal tide:					
Luni - solar	K_1	15.04107	23.93	0.72921	58
Principal lunar	O_1	13.94304	25.82	0.67598	42

TABLE 5. AMPLITUDE a (cm), PHASE κ (deg) OF MAJOR TIDAL CONSTITUENTS.

S. No.	Place	Location N	E	M_2-Tide cm	deg.	S_2-Tide cm	deg.	K_1-Tide cm	deg.	O_1-Tide cm	deg
1.	Hab River	24°.54'	66°.39'	81.46	170.25	31.76	194.92	39.24	347.75	23.57	342.89
2	Knoff Head	24.52	66.40	81.23	169.61	32.15	195.33	39.35	347.71	23.64	342.84
3.	Cape Monze	24.50	66.42	80.63	168.03	32.75	194.07	39.49	347.59	23.63	342.63
4.	Bol	24.51	66.45	81.46	167.67	33.53	196.42	39.47	347.40	23.96	342.78
5.	Buleji Point	24.50	66.49	81.93	167.52	33.60	196.44	39.34	347.18	24.01	342.84
6.	Howakes Bay Point	24.51	66.51	83.21	167.50	33.62	196.14	39.23	196.14	24.08	342.94
7.	Howakes Bay East	24.49	66.56	82.45	167.27	33.08	195.30	39.37	347.12	24.04	342.90
8.	Manard Point	24.47	66.59	82.19	167.24	33.21	195.54	39.64	347.29	24.00	342.71
9.	Karachi 1	24.48	66.59	81.22	167.33	33.36	194.86	39.81	347.46	23.97	342.75
10.	Karachi 2	24.49	66.59	81.32	167.34	33.73	194.33	39.84	347.49	23.95	342.72
11.	Clifton	24.47	67.02	81.42	167.45	33.71	194.96	40.07	347.56	23.96	342.42
12.	Ghizri Creek	24.45	67.05	83.55	167.42	34.21	196.77	39.47	347.06	24.05	342.80
13.	Bundal	24.43	67.05	83.79	167.46	34.57	197.91	39.43	347.00	24.09	342.71
14.	Bundal South	24.40	67.07	83.07	167.64	34.53	196.89	39.54	347.20	24.07	342.60
15	Phitti Creek	24.41	67.08	83.10	169.19	34.68	196.17	39.48	348.07	24.05	343.11
16.	Miran	24.38	67.09	82.29	168.67	34.85	196.13	39.59	347.71	24.17	342.68
17.	Kuddi North	24.37	67.10	82.50	169.28	34.68	196.17	39.73	348.85	24.11	342.87
18.	Kuddi South 1	24.35	67.10	82.95	168.42	35.19	195.06	39.95	347.81	24.36	342.45
19.	Kuddi South 2	24.33	67.11	82.62	166.60	36.13	192.21	40.00	346.65	24.49	341.70
20.	Khai Cr. North	24.32	67.12	81.62	165.77	35.97	190.02	40.07	346.52	24.44	341.39

TABLE 6. COMPARISON OF COMPUTED IN PREVIOUS MODEL (C_1) AND PRESENT MODEL (C_2) AMPLITUDE a (cm) PHASE κ (deg) OF MAJOR TIDAL CONSTITUENTS.

No.	Tidal constiuent Place	N	E		M_2 C_1	M_2 C_2	S_2 C_1	S_2 C_2	K_1 C_1	K_1 C_2	O_1 C_1	O_1 C_2
1	Cape Monze	24°. 50'	66°. 40'	a	79.22	80.63	31.89	32.75	38.97	39.49	23.68	23.63
				κ	167.51	168.03	193.19	194.07	347.04	342.64	342.64	342.63
2	Howakes	24.51	66.51	a	80.00	82.45	33.17	33.08	39.43	39.37	23.92	24.04
				κ	167.47	167.27	192.14	195.30	346.73	347.12	342.37	342.90
3	Karachi	24.48	66.59	a	81.00	81.22	34.10	33.73	39.73	39.81	24.11	23.97
				κ	167.47	167.33	191.67	194.33	346.65	347.46	342.25	342.75
4	Kuddi	24.35	67.11	a	82.11	82.50	36.34	35.19	39.96	39.95	24.24	24.36
				κ	167.94	169.28	191.05	195.06	345.95	347.81	341.65	342.45

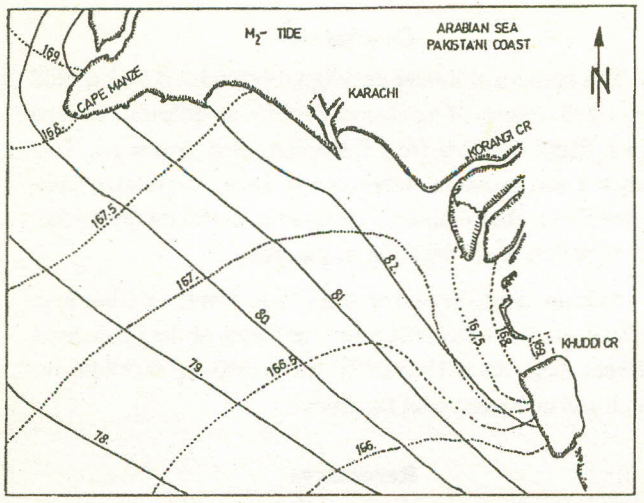

Fig. 4. M_2-tide in the Pakistani Coast Area. Co-range lines (_____) in cm and co-tidal lines (_ _ _ _)in degree.

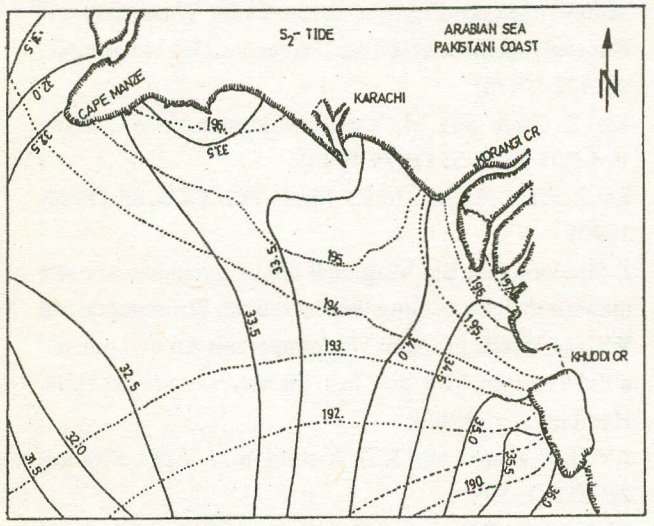

Fig.5. S_2-tide in the Pakistani Coast Area.

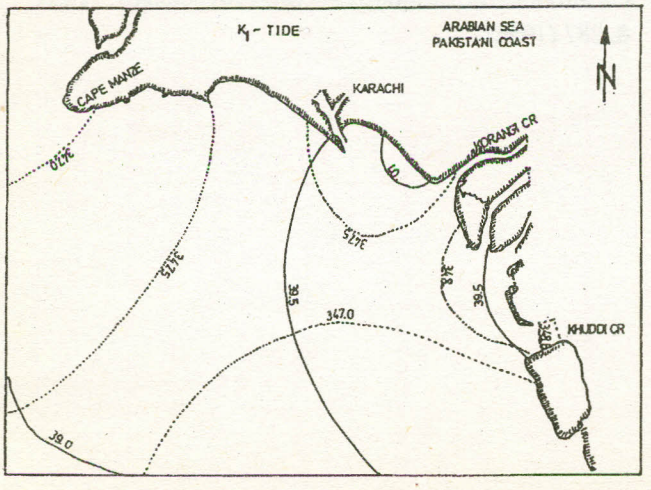

Fig.6. K_1-tide in the Pakistani Coast Area.

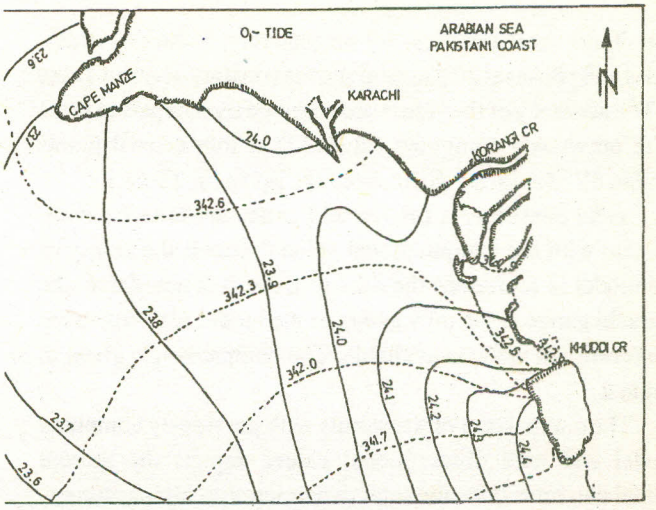

Fig. 7.O_1-tide in the Pakistani Coast Area.

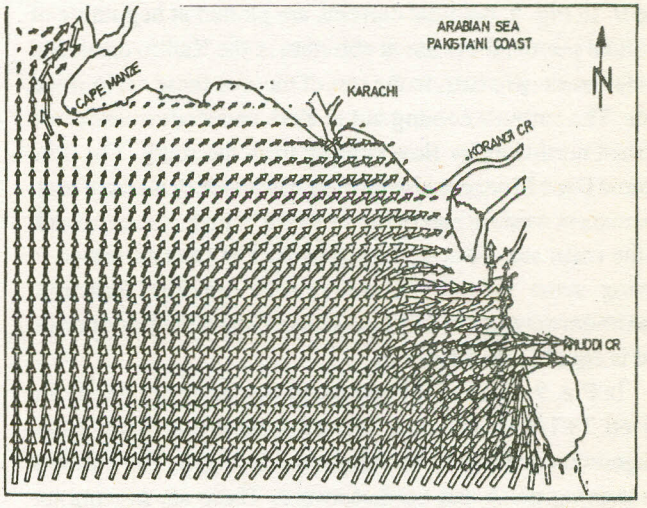

Fig.8. Tidal currents in the beginning of the tidal period of M_2-tide.

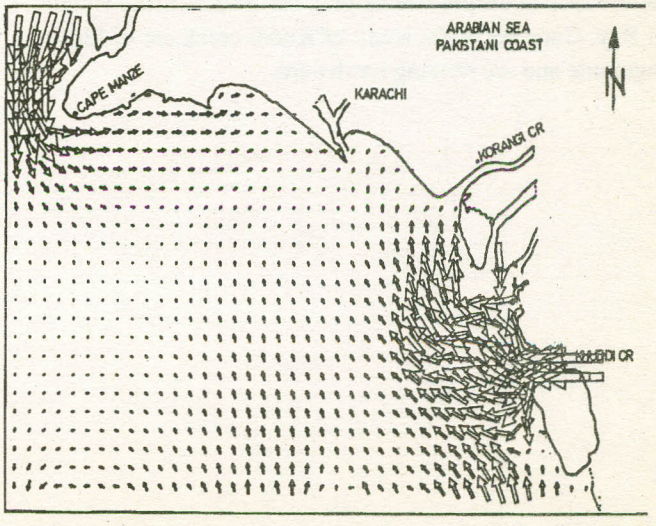

Fig.9. Tidal currents in the beginning of first quarter of the period of M_2-tide.

and O_1 are shown in Figs. 4-7 respectively. Values of amplitudes and phases at 20 places along the coast are given in Table 5. The accuracy of the values are accessed by comparing these with previously computed values [2] at four coastal points (Table 6). Maximum differences are given in Table.1.

Tidal constituents for Karachi gauge are used for comparison with the computational value to assess the ability of the model to reproduce the tidal process. It is noted that the Karachi gauge is the only gauge in the model area where the observational value is available. The comparison is given in Table.2.

The comparison of the results with previously computed model and with observational values depicts the present model can reproduce the tidal dynamics with high accuracy.

Tidal currents of M2 - tide. Tidal currents for M2-tide which is the largest partial tide (Table 4), are given in Figs. 8 and 9. In Fig. 8, the tidal currents are plotted at beginning of the tidal period, these are in ebb state in the Kadiro creek and Kuddi creek whereas, in the rest of the area these are in flood state. The currents coming out of Kudi and Kadiro creeks are pushed northwars by flow coming from the south. The flow around Cape Monze is also moving eastwards to Karachi port. Currents in western part of the southern boundary moves back to the main sea. Flow pattern after half of the tide period is having same magnitude and exactly opposite direction. Maximum magnitude of the current occurs in the Kuddi creek and is equal to 26.5 cm/sec.

In Fig. 9, the tidal current are plotted after quarter of the period T+T/4 of M2-tide. The currents are in flood state. Magnitudes are higher than appeared in Fig. 8. The currents are moving north and northeastward. These are moving towards Kadiro, Kuddi creeks and Karachi port. Current in the western strip in the plot are moving northwards to the Sonmiani Bay. Currents in the south of Kuddi creek are of higher magnitude and are moving northward.

Conclusion

The numerical model developed provides detailed tidal charts and values of tidal constituents at different coastal points. Tidal currents for M_2-tide are also presented. This study not only provides elaborated picture of the tidal dynamics, but also makes available information useful for the prediction of pollution propagation in the area.

Acknowledgement. I would like to thank the Chairman Department of Mathematics and the Dean of the College of Science, King Saud University for providing excellent research and computational facilities.

Rererences

1. Kh. Z. Elahi, Brechnung von lokalen Gezeitenphanaomenen in einem gebiet mit geringem Beobachtungsmaterial mit anwendung auf die Sonmianni Bucht (Pakistan), Mitteilangen des Franzius-Institutes fur Wasserbau and Kunsten Ingenieurwesen der Universitat Hannover, Heft., **48**, 172 (1978).
2. Kh. Z. Elahi and M. Shafique, Punjab.Univ.J. Math. Vol. **XII-XIII**, 55 (1979-1980).
3. Kh. Z. Elahi, Punjab.Univ.J. Math. Vol. **XXII**, 85, (1989-1990).
4. J. Sundermann, Ein Vergleich der analytischen and der numerischen Berechung Winderzeugter Stromungen and Wasseerstande in einem Modelmeer mit Anwen-dungen auf die Norsee, Mitt. des. Inst. fur Meerskunde der Univ. Hamburg, IV (1966).
5. J.V.U. Neumann and R.D. Richtmyer, J. Appl. Physics, **21**, 232 (1950).
6. W. Hansen, Theoriezur Errechung es Wasserstans und der Stromung in Randmeeren nebst Anwendungen, Tellus, **8**, 287 (1956).